

## Evanescence field at nanocorrugated dielectric surface

S. N. Volkov,<sup>1</sup> A. E. Kaplan,<sup>1,a)</sup> and K. Miyazaki<sup>2</sup>

<sup>1</sup>Department of Electrical and Computer Engineering, Johns Hopkins University, Baltimore, Maryland 21218, USA

<sup>2</sup>Institute of Advanced Energy, Kyoto University, Gokasho, Uji, Kyoto, 611-0011, Japan

(Received 24 September 2008; accepted 6 January 2009; published online 26 January 2009)

We study coupling of laser pulses to an evanescent electric field at a nanocorrugated dielectric surface. We find that the local electric field is increased in the surface grooves, up to a factor of 2, compared to the incident field, thus providing a positive feedback for localized subthreshold ablation, and enabling the corrugation growth. © 2009 American Institute of Physics.

[DOI: 10.1063/1.3075055]

Recently discovered laser-induced surface corrugation is now a subject of extensive investigation.<sup>1,2</sup> The subwavelength grooves emerging on the surface of solid-state films are nearly periodic nanostructures aligned normally to the linear polarization of femtosecond laser pulses. The physical mechanism of the phenomenon is still unclear. The importance of the subject is in part due to potential applications of nanostructures with controlled growth, such as nanoscale computer components, diffraction gratings, and reflectors for extreme UV and soft x rays, polarization-sensitive elements for those domains, fluence-measurement tools for femtosecond pulses, etc.

The well known regular ripples<sup>3</sup> formed by much longer nanosecond laser pulses, each exceeding the ablation threshold, under normal incidence have spacing of the order of the laser wavelength  $\lambda$ . A common physical model<sup>4</sup> for the effect is the interaction of the incident light with the standing “surface-scattered wave” of the *same wavelength*. The major differences between this phenomenon and the formation of sub- $\lambda$  nanogratings are that in the latter case laser pulses are much shorter and each of them has a subablation energy fluence.<sup>1,2</sup> This greatly emphasizes the role of inhomogeneity in the intensity distribution over the corrugated surface in the sub- $\lambda$  case.

We demonstrate here the importance of the electric-field distribution at a nanoscale corrugated surface, which may create the feedback mechanism for the growth of the sub- $\lambda$  “ripples.” Indeed, we show that an evanescent field is stronger in the grooves than at the ridges and thus may induce a localized ablation only at the bottom of grooves. The grooves then deepen with each laser shot, creating the positive feedback for the ablation process. In the growth of nanogratings, the structure itself becomes instrumental in coupling the incident light into a strong evanescent surface field, closely mimicking the structure’s spacial profile. Two factors are important here: (i) only the gratings aligned normally to the laser polarization get strong positive feedback and (ii) the phase of the evanescent field is such that the *total* field is strongest in the grooves and weakest at the ridges. The latter condition enables a shot-to-shot “amplification” of the grooves by “chiseling away” the material at their bottoms, where the local intensity exceeds a certain ablation threshold, even if the incident laser light is under threshold, while the

ridges are not much affected. The resulting corrugation period  $\Lambda$  under favorable conditions can take on *any* spatial period including  $\Lambda \ll \lambda$ . The mechanism of formation of subwavelength ripples with such short  $\Lambda$  could be, in general, different for different media, such as diamondlike carbon (DLC), TiN, SiC, and InF.<sup>1,2</sup> Our results, to be published elsewhere, show that at least for DLC, the most likely mechanism is a nanoscale instability of the surface due to large and rapid thermoplastic expansion of a surface layer assisted by phaselike transition in carbon. This instability is then further amplified and self-organized into nanoripples by the evanescent field due to the process described here. We stress, however, that regardless of material-related aspects, the amplifying mechanism via sub- $\lambda$  evanescent wave remains the near-field interaction, substantially different from that of formation of regular  $\sim \lambda$  ripples of Refs. 3 and 4.

Electromagnetic properties of corrugated surfaces with  $\Lambda \ll \lambda$  have been investigated (mostly numerically) in many works (see e.g. in Ref. 5), with the focus on (far-field) reflectivity and transmittivity properties and little attention to the field distribution at the surface itself. While near-field results can be used to explore far-field characteristics, the inverse is not true. Most of the far-field results were obtained by assuming that, instead of lateral corrugation, the boundary is formed by a smooth change of the material density in the direction normal to the surface. This approach cannot adequately describe the near-field area.

In this letter we find the local distribution of the evanescent field at a corrugated surface with a given spatial period  $\Lambda \ll \lambda$ , and with a laser beam incident normally to the surface. We demonstrate that when the beam is linearly polarized normally to the grating (i.e. along its spatial period), a highly uneven local distribution of the electric field at the surface ensues, with much higher local intensity at the bottoms of the grooves, enough to provide a positive feedback for the structure growth. Our findings are in line with the experimental results and provide a quantitative model for the localized-ablation mechanism of nanoripples formation.

We consider a laser beam incident in the negative  $y$  direction on a periodically corrugated surface with a grating wave vector  $\mathbf{K} = 2\pi\hat{\mathbf{e}}_x/\Lambda$ . The surface is an interface between two semi-infinite dielectrics with the dielectric constants  $\epsilon_1$  (the “upper” dielectric) and  $\epsilon_2$  (the “substrate”). Since  $\Lambda \ll \lambda$ , the incident beam can be treated as a plane wave, so that everything is uniform in the  $z$  direction, resulting in a two-dimensional (2D) (cylindrical) problem geometry (see

<sup>a)</sup>Electronic mail: sasha@striky.ece.jhu.edu.

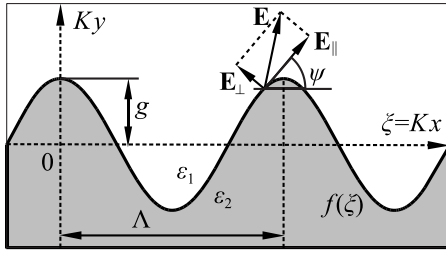


FIG. 1. Geometry of the problem.

Fig. 1). The  $\Lambda \ll \lambda$  case leads to a quasistatic problem, hence the magnetic field can be neglected, while the electric field will follow from the solutions of 2D Laplace equations for the dc potential  $U$  in each of the materials,

$$\partial^2 U / \partial x^2 + \partial^2 U / \partial y^2 = 0. \quad (1)$$

This quasistatic approach has been verified by us by also running computer simulations using a full electromagnetic (EM) wave model (see below), which showed full consistency with quasistatic approximation within the domain of convergence of the numerical solution. In the case of low reflectivity (as for the films in the experiments<sup>2</sup>), we assume that the quasistatic field far from the surface ( $|y| \gg \Lambda$ ) is constant and coincides with the incident laser field,  $E_L = E_0$ . One can readily show that if  $\mathbf{E}_L$  is normal to the grating (i.e.  $\mathbf{E}_L \parallel \mathbf{K}$ ), then it is coupled to the evanescent surface wave, whereas this is not so for  $\mathbf{E}_L \perp \mathbf{K}$ . Thus, we will only consider the case of  $\mathbf{E}_L \parallel \mathbf{K} \parallel \hat{\mathbf{e}}_x$ , so that the following static formulae hold for the electric field near the corrugated surface:

$$E_x = -\partial U / \partial x, \quad E_y = -\partial U / \partial y, \quad E_z = 0. \quad (2)$$

We assume sinusoidal corrugation of the boundary,

$$Ky_{\text{bnd}} = f(\xi) \equiv g \cos(\xi), \quad \text{with } \xi = Kx. \quad (3)$$

Because of the lateral periodicity of boundary, the same is true for the fields in both ‘‘upper’’ and ‘‘substrate’’ dielectrics, i.e.  $U + E_0 x = -\sum u_n(y) \sin(n\xi)$ . The Fourier coefficients  $u_n(y)$  for the spatial harmonics are found from Eq. (1) as  $u_n(y) = C_n \exp(\pm nKy)$ , where  $C_n$  are integration constants. By using Eq. (2), we find the fields in both subspaces,

$$\frac{1}{E_0} \begin{bmatrix} E_x^{(1)} \\ E_x^{(2)} \end{bmatrix} = 1 + \sum_{n=1}^{\infty} \begin{bmatrix} A_n e^{-nKy} \\ B_n e^{nKy} \end{bmatrix} \cos(n\xi),$$

$$\frac{1}{E_0} \begin{bmatrix} E_y^{(1)} \\ E_y^{(2)} \end{bmatrix} = \sum_{n=1}^{\infty} \begin{bmatrix} -A_n e^{-nKy} \\ B_n e^{nKy} \end{bmatrix} \sin(n\xi). \quad (4)$$

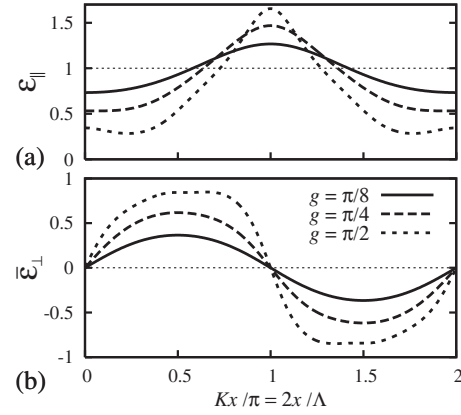
Here the superscripts (1,2) denote fields in the upper dielectric and the substrate, respectively, and the coefficients  $A_n$  and  $B_n$  are to be found from the boundary conditions at  $y = y_{\text{bnd}}(x)$ ,

$$E_{\parallel}^{(1)} = E_{\parallel}^{(2)} \quad \text{and} \quad \epsilon_1 E_{\perp}^{(1)} = \epsilon_2 E_{\perp}^{(2)}, \quad (5)$$

where the subscripts ‘‘||’’ and ‘‘⊥’’ designate field components tangential and normal to the boundary, respectively (see Fig. 1). They are

$$E_{\parallel} = E_x \cos \psi + E_y \sin \psi, \quad E_{\perp} = -E_x \sin \psi + E_y \cos \psi \quad (6)$$

at each side of the boundary, with  $\tan \psi = df/d\xi \equiv f'$ .

FIG. 2. Normalized electric fields at the corrugated boundary for  $\epsilon_2/\epsilon_1=6$ .

For convenience, we further use the normalized fields

$$\mathcal{E}_{\parallel} = \frac{E_{\parallel}^{(1)}}{E_0} = \frac{E_{\parallel}^{(2)}}{E_0}, \quad \bar{\mathcal{E}}_{\perp} = \frac{E_{\perp}^{(1)} + E_{\perp}^{(2)}}{2E_0}. \quad (7)$$

The normal fields at each side of the surface are expressed in terms of the ‘‘mean’’ amplitude  $\bar{\mathcal{E}}_{\perp}$  using Eq. (5) as

$$E_{\perp}^{(1,2)} = E_0(1 \pm \eta) \bar{\mathcal{E}}_{\perp}, \quad (8)$$

where  $\eta = (\epsilon_2 - \epsilon_1)/(\epsilon_2 + \epsilon_1)$  is a dielectric contrast factor. The upper and lower signs correspond to the upper and the substrate sides of the boundary, respectively. In the limit of a shallow grating,  $g \ll 1$ , we find

$$\mathcal{E}_{\parallel} \approx 1 - \eta f \quad \text{and} \quad \bar{\mathcal{E}}_{\perp} \approx -f'. \quad (9)$$

For relatively large modulation amplitudes  $g$ , we obtained approximate solutions for  $\mathcal{E}_{\parallel, \perp}$ ,

$$\mathcal{E}_{\parallel} \approx \frac{1 - F}{\sqrt{1 + (f')^2}} \quad \text{and} \quad \bar{\mathcal{E}}_{\perp} \approx -\frac{f' \exp(-F^2/2)}{\sqrt{1 + (f')^2}}, \quad (10)$$

where  $F = \eta \tanh(f)$ . The profiles  $\mathcal{E}_{\parallel}(\xi)$  and  $\mathcal{E}_{\perp}(\xi)$  are plotted according to Eq. (10) in Fig. 2 for different depths  $g$  and for the ratio  $\epsilon_2/\epsilon_1=6$  close to that of an air-diamond interface. In the experiments,<sup>1,2</sup>  $\epsilon_2$  ranges from  $\sim 3$  for sapphire to  $\geq 10$  for semiconductors in the near infrared, so our choice of  $\epsilon_2$  is in the middle of this wide range. We found that for  $1 < \epsilon_2/\epsilon_1 \leq 10$  the approximate solutions (10) are consistent with the results of our numerical simulations up to  $g = \pi/2$ , which corresponds to the total corrugation depth of  $\Lambda/2$ , providing thus the range of depths exceeding those observed in Refs. 1 and 2. We also found that the approximation (10) still gives a good overall prediction of the numerically generated field profiles, especially the one for  $\bar{\mathcal{E}}_{\perp}$ , up to  $g \approx 2\pi$  (the total depth of  $2\Lambda$ ).

We used two different methods to numerically model our problem. In the first method, we used the MPB package,<sup>6</sup> based on a plane EM-wave expansion for solving the Maxwell equations. The 2D problem was solved with periodic boundary conditions, after applying periodic continuation in the  $y$  direction and choosing a small wave vector  $\mathbf{k} \parallel \hat{\mathbf{e}}_y$  with  $k \equiv 2\pi/\lambda \ll 2\pi/\Lambda$ . The resulting numerical solution gets fairly noisy at higher  $g$  (up to  $\sim 20\%$  of the maximum field value at  $g = \pi/2$ ). Our second, quasistatic numerical approach was to solve Eq. (4) truncated to a finite number of coefficients  $A_n$  and  $B_n$ ; it works well for  $g \leq 1$ , with the results having much less noise compared to the MPB-based

approach, but it becomes divergent at  $g \geq \pi/2$  if  $\epsilon_2/\epsilon_1 \geq 2$ . After averaging out the noise in the MPB-method, its agreement with the quasistatic approach as well as with Eq. (10) reaches just a few percents of the maximum field value at  $g = \pi/2$  and is much better at smaller  $g$ .

At the bottoms of the grooves and at the ridges where  $f' = 0$ , we have  $E_{\perp} = 0$ , and the tangential fields at those points [Eq. (10)] are

$$(\mathcal{E}_{\parallel})_{\text{bott,ridge}} = 1 \pm \eta \tanh(g), \quad (11)$$

where the “+” sign corresponds to the bottoms (maxima) (e.g.  $\xi = \pi$ ), and “−” sign to the ridges (e.g. at  $\xi = 0$  or  $\xi = 2\pi$ ), respectively. If  $\epsilon_2/\epsilon_1 \gg 1$ , as e.g. for air-diamond or air-semiconductor boundaries, the ratio of the field amplitudes at the bottom and at the ridge can be significant. The most important fact, however, is that  $E_{\parallel}$  in the grooves can substantially exceed the incident field (up to a factor of 2), which has significant consequence to ablation processes. Even if the incident field intensity  $E_0^2$  is lower than the characteristic ablation intensity,  $E_{\text{abl}}^2 \propto F_{\text{abl}}/\tau_p$  (where  $F_{\text{abl}}$  is the critical ablation fluence and  $\tau_p$  is the laser pulse duration), the field at the bottom can exceed  $E_{\text{abl}}$  and, by selectively heating and chiseling away atoms from there, make the grating grow deeper. According to Eq. (10), as the depth  $g$  of the grating increases, the sizes of the areas with high  $E_{\parallel}$  become smaller, which results in stronger localization of ablation near the lowest points of the grooves.

A strong normal component of the electric field  $E_{\perp}$  on the groove slopes may provide an additional mechanism of grating growth. If  $E_{\perp}$  is strong enough, the electrons accelerated normally to the corrugated surface may be ejected from the dielectric and then re-enter it in the next half period of the light wave, hitting and ejecting atoms from the surface.

In conclusion, we have shown that the coupling of the incident laser light to an evanescent quasistatic electric field via a surface nanograting can be a potential mechanism of

formation of nanogratings on a dielectric surface by femto-second laser pulses. The strongest surface field, exceeding the incident field by up to a factor of 2, occurs at the bottoms of the grooves, while the field at the ridges is weaker than the incident field. The resulting contrast in the field can promote subablation growth of the grating due to preferential localized ablation at the bottoms.

The work by A.E.K. and S.N.V. is supported by AFOSR.

- <sup>1</sup>H. Varel, M. Wöhmer, A. Rosenfeld, D. Ashkenasi, and E. E. B. Campbell, *Appl. Surf. Sci.* **127**, 128 (1998); A. M. Ozkan, A. P. Malshe, T. A. Railkar, W. D. Brown, M. D. Shirk, and P. A. Molian, *Appl. Phys. Lett.* **75**, 3716 (1999); J. Bonse, H. Sturm, D. Schmidt, and W. Kautek, *Appl. Phys. A: Mater. Sci. Process.* **71**, 657 (2000); Q. Wu, Y. Ma, R. Fang, Y. Liao, Q. Yu, X. Chen, and K. Wang, *Appl. Phys. Lett.* **82**, 1703 (2003); A. Borowiec and H. K. Haugen, *ibid.* **82**, 4462 (2003); F. Costache, M. Henyk, and J. Reif, *Appl. Surf. Sci.* **208**, 486 (2003); T. Q. Jia, H. X. Chen, M. Huang, F. L. Zhao, J. R. Qiu, R. X. Li, Z. Z. Xu, X. K. He, J. Zhang, and H. Kuroda, *Phys. Rev. B* **72**, 125429 (2005); T. Tomita, K. Kinoshita, S. Matsuo, and S. Hashimoto, *Jpn. J. Appl. Phys., Part 2* **45**, L444 (2006); J. Gottmann and R. Wagner, *Proc. SPIE* **6106**, 372 (2006).
- <sup>2</sup>N. Yasumaru, K. Miyazaki, and J. Kiuchi, *Appl. Phys. A: Mater. Sci. Process.* **76**, 983 (2003); **79**, 425 (2004); **81**, 933 (2005); K. Miyazaki, N. Maekawa, W. Kobayashi, M. Kaku, N. Yasumaru, and J. Kiuchi, *ibid.* **80**, 17 (2005); G. Miyaji and K. Miyazaki, *Appl. Phys. Lett.* **89**, 191902 (2006).
- <sup>3</sup>M. Birnbaum, *J. Appl. Phys.* **36**, 3688 (1965); M. Siegrist, G. Kaech, and F. K. Kneubühl, *Appl. Phys. (Berlin)* **2**, 45 (1973); D. C. Emmony, R. P. Howson, and L. J. Willis, *Appl. Phys. Lett.* **23**, 598 (1973); J. F. Young, J. S. Preston, H. M. van Driel, and J. E. Sipe, *Phys. Rev. B* **27**, 1155 (1983), and references therein.
- <sup>4</sup>Z. Guosheng, P. M. Fauchet, and A. E. Siegman, *Phys. Rev. B* **26**, 5366 (1982); J. E. Sipe, J. F. Young, J. S. Preston, and H. M. van Driel, *ibid.* **27**, 1141 (1983).
- <sup>5</sup>R. A. Hurd, *Can. J. Phys.* **32**, 727 (1954); R. S. Elliott, *IRE Trans. Antennas Propag.* **2**, 71 (1954); S. M. Rytov, *J. Exp. Theor. Phys.* **29**, 605 (1955); *Electromagnetic Theory of Gratings*, edited by R. Petit (Springer, Berlin, 1980); I. M. Fuks, *IEEE Trans. Antennas Propag.* **49**, 630 (2001).
- <sup>6</sup>MIT Photonic-Bands Package as described in S. G. Johnson and J. D. Joannopoulos, *Opt. Express* **8**, 173 (2001).